Available online at www.sciencedirect.com
ScienceDirect
Journal of the European Ceramic Society 30 (2010) 129–138
www.elsevier.com/locate/jeurceramsoc

Fabrication and mechanisms of densification of ZrB_2-based ultra high temperature ceramics by reactive hot pressing

Lingappa Rangaraj [a], Canchi Divakar [a], Vikram Jayaram [b,*]

[a] *Materials Science Division, National Aerospace Laboratories (CSIR) Bangalore 560 017, India*
[b] *Department of Materials Engineering, Indian Institute of Science, Bangalore 560 012, India*

Received 3 March 2009; received in revised form 31 July 2009; accepted 6 August 2009
Available online 17 September 2009

Abstract

Dense ZrB_2–SiC (25–30 vol%) composites have been produced by reactive hot pressing using stoichiometric Zr, B_4C, C and Si powder mixtures with and without Ni addition at 40 MPa, 1600 °C for 60 min. Nickel, a common additive to promote densification, is shown not to be essential; the presence of an ultra-fine microstructure containing a transient plastic ZrC phase is suggested to play a key role at low temperatures, while a transient liquid phase may be responsible at temperatures above 1350 °C. Hot Pressing of non-stoichiometric mixture of Zr, B_4C and Si at 40 MPa, 1600 °C for 30 min resulted in ZrB_2–ZrC_x–SiC (15 vol%) composites of ~98% RD.

Keywords: Reactive hot pressing; Composites; Borides; Carbides; Ultra high temperature ceramics; Densification

1. Introduction

Refractory transition metal borides, such as zirconium diboride (ZrB_2) and hafnium diboride (HfB_2), with extremely high melting temperatures (>3050 °C), have been referred to as ultra high temperature ceramics (UHTCs). These materials are proposed to be used at temperature in excess of 1900 °C. However, monoliths of these materials do not withstand temperatures in excess of 1200 °C under oxidizing conditions due to the formation of ZrO_2/B_2O_3 layers. Addition of SiC to ZrB_2/HfB_2 materials improves oxidation resistance up to 1500 °C, by formation of SiO_2 which leads to a more stable and impervious borosilicate glass layer.[1–9] Such materials have been proposed for sharp leading edges on re-entry vehicle applications, because of their relatively good oxidation and erosion resistance in hostile environments.[10] The family of UHTCs developed by NASA for SHARP hypersonic aero-thermodynamic research probe-ballistic experiments 1 and 2 (SHARP-B1 and SHARP-B2) have been tested under arc-jet conditions.[11] Thermo-structural designs of critical parts of re-entry vehicles such as nose cap and wing leading edges have been tested and validation is under progress for flight conditions.[12]

Because of the extremely high melting temperatures of these materials, usually sintering temperatures of ~2000 °C are needed to produce dense materials. There have been many methods to densify ZrB_2 and HfB_2 based composites.[9,11,13–42] Pressureless sintering (PS) has been shown to achieve relative densities ~94% at 1800 °C in the presence of Fe and Cr impurities,[13,14] while additions of C and B_4C to ZrB_2 have enabled the production of >99% RD at 1900 °C owing to the reduction of surface oxides of ZrO_2/B_2O_3 which would have otherwise melted and led to grain coarsening and consequent retardation of sintering.[15,16] High RD has also been achieved through additions of $MoSi_2$ to ZrB_2 at 1850 °C[17–19] while the addition of SiC (20 wt%) and Mo (4 wt%) to ZrB_2 required temperatures ~2200–2250 °C.[20] Hot pressing of ZrB_2–SiC composites using ZrB_2 and SiC powder mixtures have produced ~98% RD with various sintering additives.[9,11,21–30] The addition of $TaSi_2$ reduced the densification temperature to 1600 °C,[23] while Ni additions enabled 98% RD at 1850 °C[31,32] though with the penalty that softening of the metal led to catastrophic failure at temperatures higher than about 1000 °C even at low stresses.

In recent years reactive hot pressing (RHP) has been used to produce ZrB_2–SiC composites including uniaxial pressing

* Corresponding author. Tel.: +91 080 22933243; fax: +91 080 23601198.
E-mail address: qjayaram@materials.iisc.ernet.in (V. Jayaram).

0955-2219/$ – see front matter © 2009 Elsevier Ltd. All rights reserved.
doi:10.1016/j.jeurceramsoc.2009.08.003

of Zr/ZrH_2–B_4C–Si powder reactant mixtures[33–38] and spark plasma sintering (SPS) of boride-based ceramic composites[39,40] at 1900 °C. The mechanisms of densifications were not clear. Attrition milling of elemental Zr–B, with SiC (20 vol%), and a small amount of B_4C powder mixture yielded ZrB_2–SiC composites at 1700 °C.[38] The formation of fine ZrB_2 and the elimination of oxide impurities using B_4C were key factors that enabled high density at 1700 °C. Most recently, a combination of SPS and reactive synthesis produced ~98.5% RD ZrB_2–SiC composites at 1450 °C though, once again, the mechanism of densification was not clear.[41] Recent work on vacuum RHP of ZrB_2–SiC–ZrC composites using a planetary ball milled Zr, Si and B_4C mixture led to 97.3% RD at 1600 °C after 3 h.[42] These samples are treated at 1450 °C for 3 h before reaching the final temperature. The densification was attributed to the planetary ball milling which creates the defects in the starting materials and removal of oxide impurities.

Our recent work showed that dense $2ZrB_2$–ZrC (97.3% RD) composites could be obtained at ~1600 °C by RHP of stoichiometric mixtures of 3Zr–B_4C powders with 1 wt% Ni (0.5 vol%).[43] The addition of Ni helps only the completion of reaction at 1200 °C, and once temperature was increased to 1400 °C or 1600 °C the reaction completes without Ni. The same work showed that the excess Zr yielded ZrB_2–ZrC_x composite with 99% RD at temperature as low as 1200 °C by exploiting the formation of a non-stoichiometric zirconium carbide (ZrC_x) which enhances the densification. In addition to the fine grained (0.43–0.64 μm) materials formed, both, reduction in flow stress as well as greatly increased diffusion coefficients were responsible for the enhanced rates of densification at low temperatures.

Thus, the present work was undertaken to extend the above route to establish the possibility of lowering the process temperature and time for ZrB_2–SiC composites by RHP of Zr, B_4C and Si in various combinations and to study the progress of reaction as a function of temperature. The effect of Ni addition on reaction and densification of ZrB_2–SiC composites is also examined.

2. Experimental procedure

The following schemes of processing were employed. In the first case, ZrB_2–SiC (25 vol%) composites were prepared from stoichiometric mixtures using the following reaction:

$$2Zr + B_4C + Si \rightarrow 2ZrB_2 + SiC \quad (1)$$

The above reaction has large negative Gibbs free energy changes ($\Delta G_{298} = -395.21$ and $\Delta G_{1873} = -342.97$ kJ/mol), showing that the reactions are thermodynamically favourable.[36,42]

In a variant of the above route, excess Si and C were added to increase the amount of SiC to 30 vol% according to reaction (2):

$$2Zr + B_4C + 1.26Si + 0.26C \rightarrow 2ZrB_2 + 1.26SiC \quad (2)$$

The expected theoretical densities of the composites in reactions (1) and (2) are 5.37 g/cm^3 and 5.23 g/cm^3, respectively.

In the second case, excess Zr was added to produce ZrB_2–ZrC_x–SiC composites according to reaction (3):

$$2.5Zr + B_4C + 0.65Si \rightarrow 2ZrB_2 + 0.5ZrC_x + 0.65SiC \quad (3)$$

with volume fractions of ZrB_2, ZrC_x and SiC being ~70%, ~14.5% and ~15.5%, respectively, and an expected theoretical density of 5.71 g/cm^3.

The composites produced according to reactions (1)–(3) will be referred as ZBSC-1, ZBSC-2 and ZBCSC, respectively, and they have been labeled in Table 1. When Ni is added, the amount corresponds to 1 wt% of the total mixture and a volume fraction ~0.5% in the final product.

2.1. Materials and processing

Commercial powders of Zr: ~98% purity (Ti-0.3%, Si-0.5%, Fe-0.2%, Ca-0.15%, Al-0.05%, H-0.2%), 2–10 μm (d_{50}: 7.52 μm) particle size (M/s Yashoda Special Metals, Hyderabad, India), B_4C: ~99% purity, ~10–20 μm (d_{50}: 11 μm) particle size (M/s Boron Carbide India Ltd., Mumbai, India), Si: 99% purity, ~4 μm particle size (M/s Elkem, Germany), graphite: ultra high purity (M/s Ultra carbon Corporation, USA) and Ni: 99.5% purity, ~4 μm particle size (M/s INCO, United Kingdom) have been used in the present study. The analysis report of the B_4C supplied by the manufacturer indicates B + C: >99%, and free carbon <1%, Fe: <0.2%, B_2O_3: <0.4%, Si: <0.091% for the B_4C powder. The required amounts of powders according to ZBSC-1, ZBSC-2 and ZBCSC with 1 wt% Ni were mixed in ethanol using a rotary ball mill with ZrO_2 (8 mol% Y_2O_3) milling media for 24 h in a plastic bottle and dried at ~100 °C for 5 h. Selected compositions without Ni addition were also mixed. The weight loss of the ZrO_2 milling media after each mixing is ~2 wt% indicating the incorporation of oxide impurity in the starting mixtures.

Since molten Si is likely to be squeezed out during RHP, the dried powder mixtures were filled in a graphite crucible with one end closed. The powder mixture was encapsulated by flexible graphite sheet to eliminate contact with the die and plungers. The powder mixture assembly was placed in a graphite die of ID-30 mm and 80 mm height. The die/powder assembly was placed in a vacuum hot press (M/s Materials Research Furnaces, Suncook, NH). After attaining a vacuum of 5×10^{-5} Torr, heating was continued at different rates from 5 to 10 °C/min. The RHP experiments were conducted in the temperature range 1400–1600 °C for 30–60 min with Ni. The application of pressure was initiated at 1200 °C and the required pressure of 40 MPa was reached in ~25 min, held for the required time and released ~10 min from the start of the cooling sequence. The details of the RHP are given elsewhere.[43,44] To understand the progress of the reaction of Zr–B_4C–Si powder mixtures, experiments have been conducted at temperatures in the range 1000–1400 °C.

In addition, specifically to monitor the progress of conversion of boron carbide, large particles of B_4C were chosen (<74 μm, M/s Sigma–Aldrich, Germany) in the ZBSC-1 starting mixture according to reaction (1). Typical experiments were conducted

Table 1
Experimental conditions, phases formed and density of the ZrB_2–SiC and ZrB_2–ZrC_x–SiC composites.

Sl. No.	Experimental conditions (MPa/°C/min)	Phases	Density (g/cm^3)
ZBSC-1: $2Zr + B_4C + Si \rightarrow 2ZrB_2 + SiC$ (25 vol%)			
1	–/1000/5 (1 wt% Ni)	ZrB_2, ZrC, ZrSi, $ZrSi_2$, Zr, B_4C, Si	2.24
2	–/1200/2 (1 wt% Ni)	ZrB_2, SiC, ZrO_2	2.34 (∼43% RD)
3	40/1400/2 (1 wt% Ni)	ZrB_2, SiC, ZrO_2	3.66 (∼68% RD)
4	40/1400/30 (1 wt% Ni)	ZrB_2, SiC	4.28 (∼80% RD)
5	40/1400/30 (1 wt% Ni)[a]	ZrB_2, SiC	4.60 (85.4% RD)
6	40/1600/30 (1 wt% Ni)	ZrB_2, SiC	5.22 (∼97% RD)
7	40/1600/60 (1 wt% Ni)	ZrB_2, SiC	5.25 (97.5% RD)
8	40/1600/30	ZrB_2, SiC, B_4C[b]	5.15
9	40/1600/60	ZrB_2, SiC	5.22 (97.4% RD)
ZBSC-2: $2Zr + B_4C + 1.26Si + 0.26C \rightarrow 2ZrB_2 + 1.26SiC$ (30 vol%)			
10	40/1600/60	ZrB_2, SiC	5.03 (96% RD)
ZBSC-1 (coarse B_4C): $2Zr + B_4C + Si \rightarrow 2ZrB_2 + SiC$ (25 vol%)			
11	40/1400/30 (1 wt% Ni)[a]	ZrB_2, SiC, ZrO_2, B_4C[b]	4.87
12	40/1600/30 (1 wt% Ni)	ZrB_2, SiC, B_4C[b]	5.04
ZBCSC: $2.5Zr + B_4C + 0.65Si \rightarrow 2ZrB_2 + 0.5ZrC_x + 0.65SiC$ (15 vol%)			
13	40/1400/30 (1 wt% Ni)[a]	ZrB_2, ZrC_x, SiC, ZrO_2	4.67 (81.7% RD)
14	40/1600/30 (1 wt% Ni)	ZrB_2, ZrC_x, SiC, ZrO_2	5.55 (97% RD)
15	40/1600/30	ZrB_2, ZrC_x, SiC, ZrO_2	5.61 (98% RD)

[a] Pressure initiated at 1000 °C and remaining samples pressure initiated at 1200 °C.
[b] Observed under SEM, RD: relative density.

at 40 MPa and 1400/1600 °C for 30 min under conditions similar to those mentioned above.

2.2. Characterization of the composites

The top and bottom surfaces of reactively hot pressed composites were ground and polished using SiC abrasive paper and diamond paste down to 0.25 μm using an automatic polishing machine (Ecomet 4000 with Automet 2000, M/s Buehler, USA) followed by ultrasonic cleaning with acetone. The bulk density measurements were performed using the Archimedes method. X-ray powder diffraction (Philips, Eindhoven, The Netherlands) was used (Cu Kα radiation) to identify the phases present in the composites. Microstructural observations of polished surfaces were made using scanning electron microscopy (SEM, FEI-Sirion, Eindhoven, The Netherlands) with energy dispersive spectroscopy (EDAX, super-ultra-thin window, Genesis Spectrum, Mahwah, NJ 07430, USA). The SiC content and porosity in the composites reported has been measured through image analysis of the SEM micrographs by the line intercept method.

3. Results

Initially, results on synthesis and densification of ZrB_2–SiC composites will be presented, followed by ZrB_2–ZrC_x–SiC composites. The experimental conditions, phases formed and densities of the ZBSC-1, ZBSC-2 and ZBCSC composites are given in Table 1.

3.1. ZrB_2–SiC composites

X-ray diffraction (XRD) patterns of the polished surfaces of the ZBSC-1 (ZrB_2–SiC: 25 vol%) composites produced at 1000–1600 °C with 1 wt% Ni are shown in Fig. 1. Starting phases (Zr, Si and B_4C) can be clearly seen after mixing for 24 h (Fig. 1A(a)). At 1000 °C for 5 min, the sample showed the formation of ZrB_2, ZrC, ZrSi, $ZrSi_2$ and ZrO_2 phases with unreacted Zr and B_4C (Fig. 1A(b)). The enlarged view of Fig. 1A(b) is shown separately in Fig. 1B. At 1200 °C for 2 min, the ZrC, ZrSi, $ZrSi_2$ lines disappear and lines corresponding to ZrB_2 and SiC (β) phases with tiny peaks of ZrO_2 were observed (Fig. 1A(c)). At 1400/1600 °C the elimination of ZrO_2 can be seen (Fig. 1A(d) and (e)). Thus, ZrB_2 and SiC phases formed via reaction of ZrC and Zr–Si compounds with the remaining B_4C at 1000–1200 °C.

The density of the composites increases from 4.28 g/cm^3 (80% RD) at 1400 °C for 30 min to 5.22 g/cm^3 (97.2% RD) at 1600 °C for 30 min and increase in holding time to 60 min resulted in only a small increase in RD to ∼98%. SEM micrographs of ZBSC-1 composites produced at 40 MPa, 1600 °C for 30 min with 1 wt% Ni and without Ni are shown in Fig. 2(a) and (b). The effect of Ni addition on final RD of the composite produced is marginal (Table 1 as well as the relative absence of porosity in Fig. 2), however the composites produced without Ni at 1600 °C for 30 min showed the presence of partially reacted B_4C particles (Fig. 2(b) and (c)), while those held at longer time (60 min) did not show any B_4C (Fig. 2(d)). Thus, the composite is able to densify in the absence of Ni despite the presence of partially reacted B_4C; this is a point that may be seen with greater clarity when the results with coarse B_4C (<74 μm) particles are presented later in this paper.

Typical SEM micrographs of the ZBSC-1 composite produced at 1600 °C for 30 min with 1 wt% Ni are shown in Fig. 3. Distribution of ZrB_2 and SiC phases are seen with no evidence for any other phases (Fig. 3(a)). The EDS plot of the SiC regions in the composite produced at 1600 °C (Fig. 3(c)) shows clearly the presence of Ni, which may be seen in Fig. 3(b) as very fine

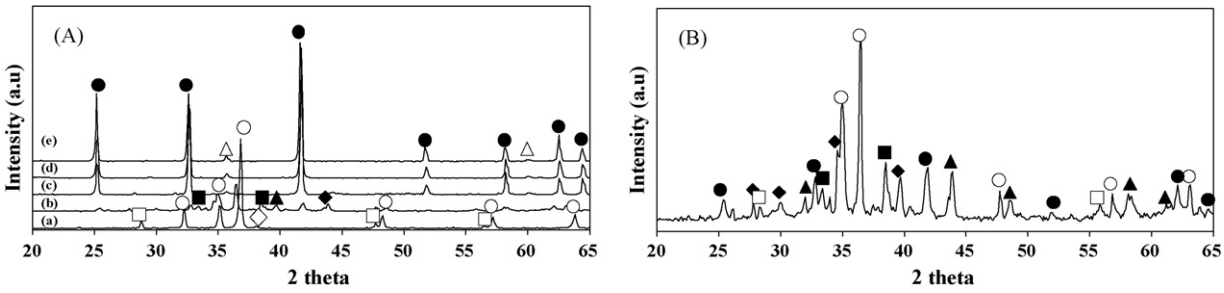

Fig. 1. The X-ray diffraction patterns of the ZBSC-1 (25 vol% SiC) composites produced with 1 wt% Ni: (a) starting 2Zr–B_4C–Si powder mixture, (b) –/1000 °C for 5 min, (c) –/1200 °C for 2 min, (d) 40 MPa/1400 °C for 2 min and (e) 40 MPa/1600 °C for 30 min (●: ZrB_2, △: SiC, ■: ZrC, ▲: ZrSi, ♦: $ZrSi_2$, ◯: Zr, □: Si and ◊: B_4C). The enlarged view of A(b) shown separately in B indicates the presence of ZrB_2, ZrC, ZrSi and $ZrSi_2$ phases.

particles. Also seen in the same figure are dark spots within the SiC regions, which are due to pores. The estimated porosity using image analysis is ∼3%, which correlates well with the measured RD (97%) of the composite. Thus, dense ZrB_2–SiC composite can be produced at 1600 °C, which is ∼250 °C lower than that reported[33,34,36,37] for Zr/B_4C/Si mixtures and ∼100 °C lower than Zr–B–SiC–B_4C,[38] with elemental Zr, B and submicron SiC (0.7 μm).

Typical SEM micrographs with EDS plot of the ZrB_2–SiC composites produced at intermediate stages of the densification process shown in Figs. 4 and 5 illustrate the phase evolution during RHP. The microstructure after 2 min at 1200 °C (without pressure) shows a fine platelet microstructure (Fig. 4(a)) with lateral dimensions that are less than 1 μm and a thickness of ∼0.1–0.2 μm. The EDS plot (Fig. 4(b)) showed the presence of Zr–B–Si–C elements. Even though the XRD (Fig. 1A(d)) showed only ZrB_2 and SiC phases, EDS analysis of the sample produced at 1400 °C shows regions of intermediate Si-rich phases (Fig. 5(a) and (c)). As the inner core of Zr–Si and residual B, C react, the outer rim of ZrB_2 (Fig. 5(b)) gradually thickens while a fine ZrB_2–SiC forms in the middle of the composite.

In order to understand the reaction sequence better, composite were prepared with coarse B_4C (>74 μm) powder with which the reaction does not proceed to completion at 40 MPa, 1400 °C for 30 min even in the presence of Ni. As shown in Fig. 6(a), despite the significant amount of unreacted B_4C, densification is substantially completed. The white regions in Fig. 6(a) correspond to ZrO_2 and the XRD patterns up to 1400 °C support such a conclusion. However, once the temperature is increased to 1600 °C, the ZrO_2 peaks disappear, presumably by carbothermal reduction by B_4C.[16,38] Incidentally, it may be noted that the presence of minor amount of oxide does not appear to affect densification, since the microstructure shown in Fig. 6 has little porosity, despite the partially reacted B_4C. As is described

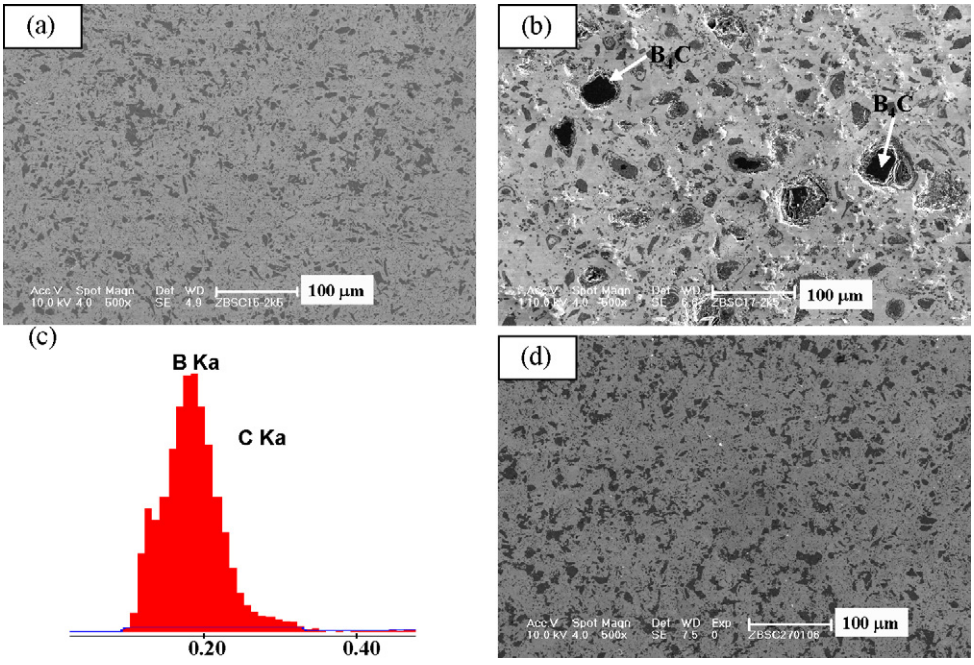

Fig. 2. SEM micrographs of ZBSC-1 (25 vol% SiC) composites produced at 40 MPa, 1600 °C (a) with 1 wt% Ni for 30 min, (b) without Ni for 30 min. The dense microstructure with uniform distribution of SiC is observed in (a) and the partially reacted B_4C particles are seen in (b). The EDS Plot of B_4C is shown in (c). Without Ni, the completion of the reaction can be seen after holding for 60 min (d).

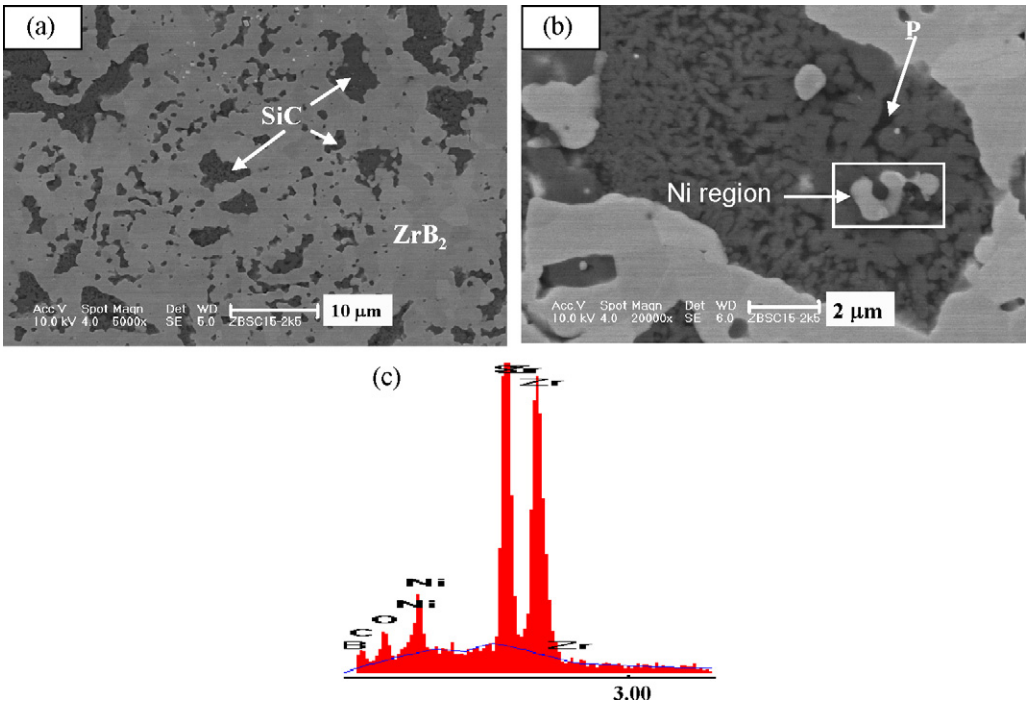

Fig. 3. SEM micrographs of ZBSC-1 (25 vol% SiC) composite produced at 40 MPa, 1600 °C for 30 min with 1 wt% Ni. The light grey and dark phases in (a) are ZrB_2 and SiC, respectively. The pores (P) may be seen within the larger SiC region in (b). The EDS plot of the light grey regions within the SiC showed the presence of Ni (c).

later in the discussion, it is possible that the major part of the carbon in a B_4C particle is converted to a single SiC region. It is possible to test this hypothesis by assuming that the outer-most ring of fine SiC corresponds to the original perimeter of the B_4C (though this is probably a slight underestimate) and comparing the areas of the section of the final SiC particle with that of the original B_4C. Such a comparison (Fig. 6(c)) yields a SiC: B_4C area ratio of 0.43 ± 0.11.

Composite (ZBSC-2) made with extra Si and C to yield 30 vol% SiC show a marginally smaller final density of 5.03 g/cm^3 (96% RD) at 40 MPa, 1600 °C for 60 min. The SEM micrograph of the composite (Fig. 7) shows a bi-modal distribution of SiC and a measured porosity of ~4% within the larger SiC agglomerates. The volume fractions of SiC in the ZBSC-1 and ZBSC-2 composites are $25.5 \pm 3.3\%$ and $30.1 \pm 5.4\%$, respectively, and are in good agreement with calculated values according to reaction (1) and (2).

3.2. ZrB_2–ZrC_x–SiC composites (ZBCSC)

The XRD patterns of the composites produced at 1400 °C and 1600 °C for 30 min are shown in Fig. 8. The observed phases are ZrB_2, ZrC_x and SiC with small peaks of m-ZrO_2 in both the cases. The density of the composites increases from 4.67 g/cm^3 (81.7% RD) at 1400 °C to 5.55 g/cm^3 (97% RD) at 1600 °C (Table 1), whereas without Ni resulted in ~98% RD at 1600 °C. These results may be contrasted with earlier reports that indicated that the densification of ZrB_2–ZrC–SiC composites by RHP[36] and SPS[39,40] required temperatures above 1800 °C. Typical back-scattered electron image of the composite with 1 wt%

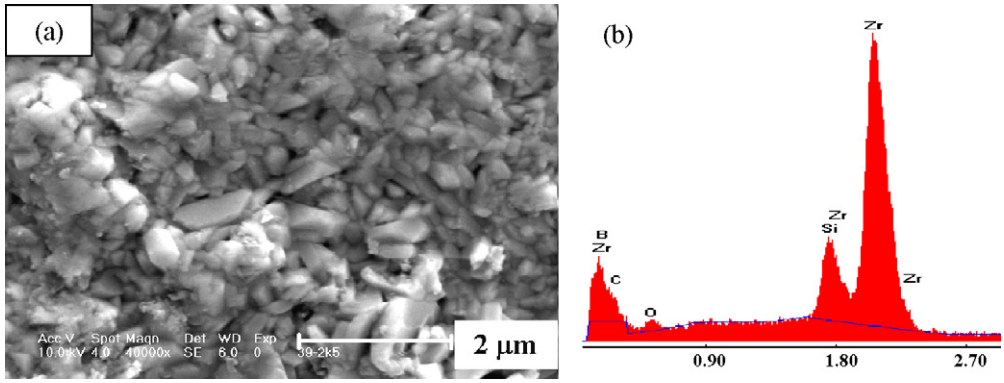

Fig. 4. SEM micrograph (a) of ZBSC-1 (25 vol% SiC) with 1 wt% Ni produced at 1200 °C for 2 min showing the very fine plate-like microstructure of ZrB_2 and SiC phases. The EDS plot (b) showed the presence of Zr–Si–B–C.

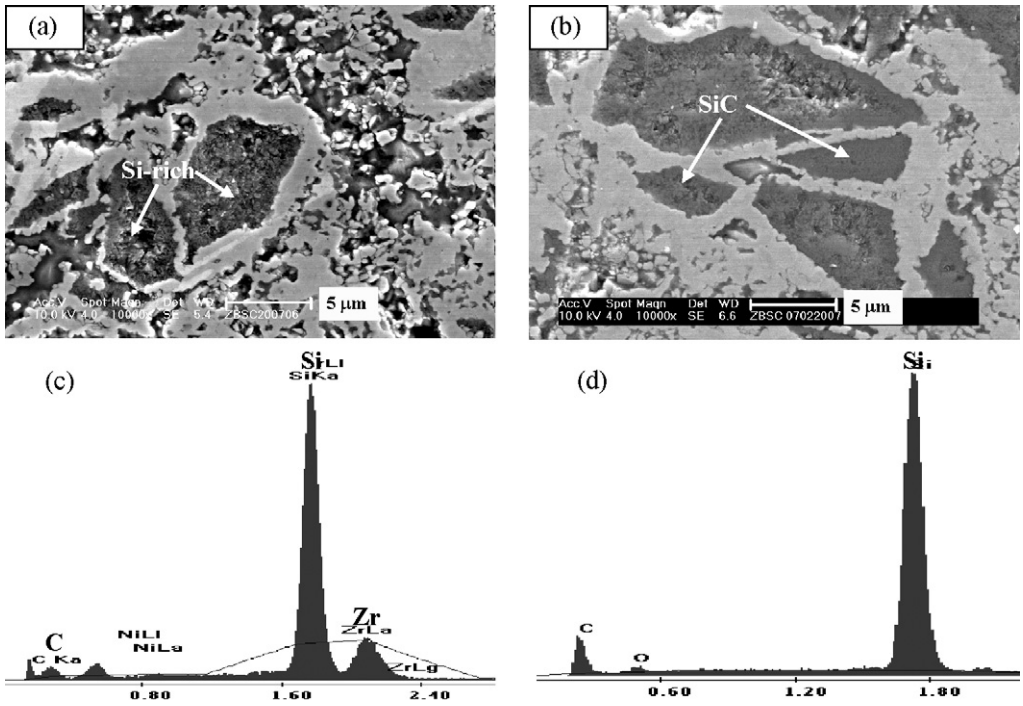

Fig. 5. SEM micrographs of ZBSC-1 (25 vol% SiC) composite produced with 1 wt% Ni at 40 MPa, 1400 °C: (a) after 2 min and (b) 30 min. (c) and (d) show corresponding EDS plots of the Si-rich regions revealing the presence of some Zr initially which disappears to yield pure SiC as time progresses.

Ni is shown in Fig. 9. The volume % of SiC estimated in the composite from image analysis is 16 ± 4. The micrograph shows the same pore distribution in the larger agglomerates of SiC as seen earlier in ZBSC-1 and ZBSC-2.

4. Discussion

We begin with a summary of the main findings, with emphasis on aspects that diverge from some earlier reports.

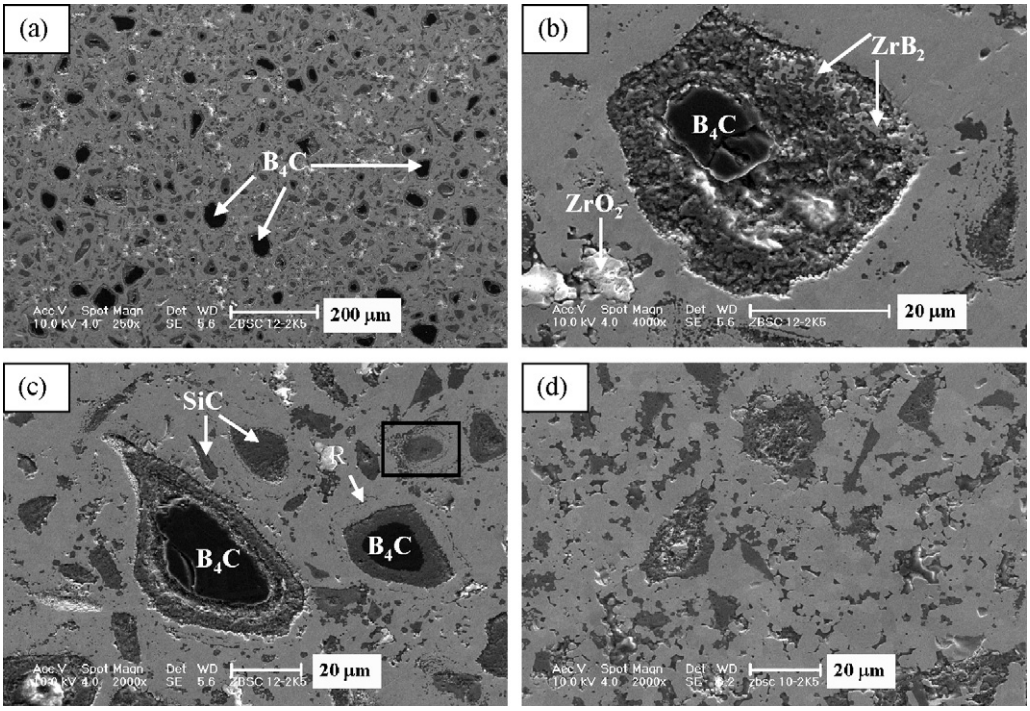

Fig. 6. SEM micrographs of ZBSC-1 (25 vol% SiC) composite (B_4C: >74 μm powder) produced with 1 wt% Ni at 40 MPa, 1400 °C for 30 min. (a) Lower magnification micrograph showed more partially reacted B_4C particles. (b) ZrB_2 regions in the former B_4C particle shown by arrows. (c) Progress of the reaction and formation of SiC ring around ZrB_2 rim (R) around B_4C particle. (d) The composite produced with 1 wt% Ni at 1600 °C for 30 min showed the elimination of B_4C and ZrO_2.

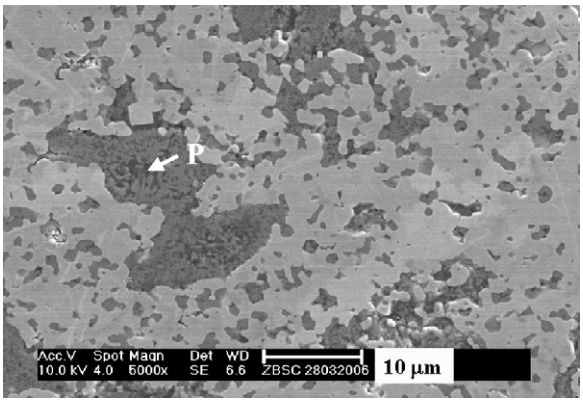

Fig. 7. SEM micrograph of the ZBSC-2 (30 vol% SiC) composite produced at 40 MPa, 1600 °C for 60 min shows the distribution of SiC within which pores are observed (P).

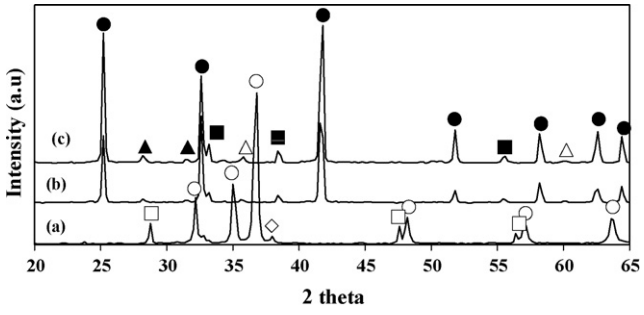

Fig. 8. The X-ray diffraction patterns of the ZBCSC composites produced with 1 wt% Ni: (a) starting 2.5Zr–B_4C–0.65Si powder mixture, (b) 40 MPa, 1400 °C for 30 min, and (c) 40 MPa, 1600 °C for 30 min (●: ZrB_2, △: SiC, ■ : ZrC_x, ▲: ZrO_2, ◯: Zr, □: Si and ◊: B_4C).

4.1. Reaction of Zr–B_4C–Si powder mixtures

Firstly, it is clear that the process of reaction of Zr–B_4C–Si to form dense ZrB_2–SiC composites does not intrinsically depend on the presence of Ni. The driving force for solid-state exchange reactions arises from the formation of thermodynamically stable final products. A possible sequence of steps resulting in reaction (1) is similar to that reported earlier in the Hf–Si–B_4C[35] and ZrH_2–Si–B_4C[37] systems. The present XRD analysis of the samples after processing at 1000 °C and 1200 °C helps to trace a possible sequence of steps that lead to reaction (1).

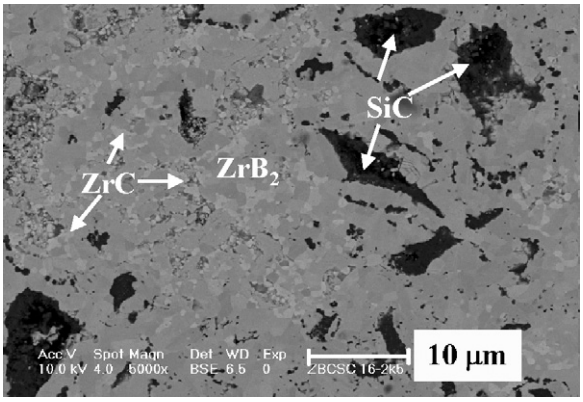

Fig. 9. Back scattered electron SEM image of the ZBCSC composite produced at 40 MPa, 1600 °C for 30 min with 1 wt% Ni showing the ZrB_2, ZrC_x and SiC phases.

At 1000 °C, the following reactions are envisaged:

$$3Zr + B_4C \rightarrow 2ZrB_2 + ZrC \quad (4)$$

$$xZr + ySi \rightarrow Zr_xSi_y \quad (5)$$

where 'x' is 1 and 'y' is either 1 or 2 for ZrSi or $ZrSi_2$.

At 1200 °C,

$$2ZrC + 3Si + B_4C \rightarrow 2ZrB_2 + 3SiC \quad (6)$$

$$ZrC + ZrSi + B_4C + Si \rightarrow 2ZrB_2 + 2SiC \quad (7)$$

$$ZrC + ZrSi_2 + B_4C \rightarrow 2ZrB_2 + 2SiC \quad (8)$$

Reactions between Zr and B_4C, and Zr and Si (Fig. 1B and reactions (4) and (5)) readily take place at temperatures ~800–1200 °C owing to the high driving forces and large diffusivities of species in Zr. In addition, because Zr is a ductile phase, one may readily envisage the formation of B_4C–Zr and Si–Zr interfaces during ball milling. In contrast, Si and B_4C are both brittle and direct reaction between them to form SiC also necessitates the formation of Si-borides which requires much higher temperature. Recent report on addition of $TiSi_2$ (0–10 wt%) to TiB_2 and Gibbs free energy calculation for forming Ti_5Si_3 and SiB_6 showed that this reaction was thermodynamically not feasible below the sintering temperature of 1645 °C.[45] At 1200 °C after 2 min, the formation of ZrB_2 and SiC (Fig. 1A(c)), are in agreement with a similar observation made during reactive sintering at 1150 °C for 2 h.[35,37]

The formation of ZrO_2 at temperature up to 1400 °C and disappearance (reduction) once the temperature is increased to 1600 °C may be described by the following reactions:

$$3Zr + B_2O_3(l) + 2C \rightarrow ZrB_2 + ZrC + ZrO_2 + CO(g) \quad (9)$$

$$2ZrO_2 + Si + B_4C + 4C \rightarrow 2ZrB_2 + SiC + 4CO(g) \quad (10)$$

The free carbon present in the starting B_4C material (1%) may be helpful for the surface reduction of oxides.

4.2. Microstructural analysis

The intermediate stages of dissolution of particles include the formation of a rim that is rich in SiC with fine interspersed particles of ZrB_2, while the majority of the ZrB_2 forms an interconnected matrix. As the reaction progresses into the B_4C, the matrix continues to coarsen through transport of the newly generated ZrB_2, presumably by transport through high diffusivity paths in the SiC (Fig. 6(b)) that are, as yet, not known, involving a liquid phase. This growth of the boride matrix periodically isolates SiC regions which appear as concentric rings of diameter ~5–10 μm around the remaining B_4C. The final result is the occurrence of a core of SiC, smaller than the size of the original B_4C, and almost entirely devoid of ZrB_2 (regions R in Fig. 6 (c)). Conversion of a B_4C particle to SiC by conservation of carbon yields a volume ratio of SiC: B_4C of 0.57, which compares

favourably with the experimental value of 0.43 ± 0.11. Once the temperature is increased to 1600 °C, the reaction completes to form clusters of SiC surrounded by ZrB_2 (Fig. 6(d)). These intermediate stages are not easily discerned in the composites made with fine B_4C (10–20 μm) in which the reaction proceeds to completion (Fig. 5).

The microstructural analysis helps in proposing the reaction mechanism as follows. As the reaction progresses, the matrix continues to coarsen through newly generated ZrB_2 presumably by transport through high diffusivity paths in the SiC. This path may involve a liquid phase and it is difficult to imagine how solid-state diffusivity in ZrB_2 and SiC could sustain coarsening at such low temperatures. The reactions between Zr and B_4C and between Zr and Si are the ones that are expected to start first at 1000 °C, as shown by others[37,41] at temperatures as low as 600 °C[38] at which all phases are expected to be in solid state. In the present case, the presence of transient ZrC and Zr–Si intermetallics at 1000 °C in the ZBSC-1 composite supports such a conclusion. Subsequent conversion of ZrC and Zr–Si intermetallics to the final product appears to occur through a mechanism wherein B_4C particles are replaced by a fine mixture of product phases (ZrB_2–SiC) from which the ZrB_2 is able to continuously attach itself to the matrix, leaving behind a SiC region that is relatively free of ZrB_2. Such a coarsening sequence implies the existence of rapid diffusion paths for Zr and B and which are most likely to be due to a liquid.

4.3. Densification of the composites

The final densities of the composites produced with and without Ni after 60 min are similar (Fig. 2(a), (d) and Table 1). A similar conclusion holds for the reaction: Ni helps to accelerate the reaction, but a slightly longer time can achieve a similar result without Ni. The densification is similarly independent of the reaction as seen in the fact that the composites made with coarse B_4C (Fig. 6) display little porosity but a significant volume fraction of partially reacted B_4C. These two aspects suggest that the features that drive densification must lie elsewhere in the properties of the matrix that is created during the reaction. In particular, the insensitivity of densification to B_4C particle size suggests that heat evolution during reaction also does not contribute significantly to promoting densification. The sample dimensions, thermal conductivity of the phases and the fact that reaction between Zr and B_4C begins at ~600–800 °C and is not complete even at 1000 °C, together suggest that adiabatic effects are not significant. Similar behaviour was observed in an earlier work[43] on RHP of Zr–B_4C mixtures in which it was shown that the absence of Ni only led to marginally larger levels of porosity and greater amounts of retained B_4C.

We infer from these observations that the formation of a fine grained ZrB_2–ZrC matrix is the key step that aids densification, particularly during the transient heating stage, even in the Si-containing materials (note that even in the ZrB_2–SiC composites, ZrC is formed initially as shown in Fig. 1B). Within this matrix, the role of ZrC assumes some importance since it is well known that the flow stresses and diffusion coefficients in transition metal carbides of ZrC and TiC drops significantly with temperature, particularly in the presence of non-stoichiometry, as has been demonstrated in deformation and densification experiments elsewhere.[43,46,47] A second factor that is likely to lead to enhanced densification is the fine grained microstructure that results from the reaction as illustrated in Fig. 4 showing platelets and particles of ZrB_2 and SiC of $\sim 0.3 \pm 0.15$ μm. Early stages of densification in Zr–B_4C mixtures at 1000 °C have shown microstructures with a length scale of 50 nm.[43] Since grain boundary diffusion processes lead to sintering rates that scale with r^4, where 'r' is a grain size, substantial enhancements in sintering rates may be expected from the microstructural refinement in reactively processed materials such as shown here or elsewhere[38] compared with those that are seen when powders of ~few μm are used, as in pressureless sintering or in hot pressing at elevated temperatures.

At higher temperatures (>1200 °C), after the equilibrium phases have formed and ZrC is no longer present, a further factor that can contribute to densification is the presence of liquid phases: Zr–Si displays a eutectic at ~1370 °C[48] and, indeed, during the present densification experiments, it is possible to observe a sudden increase in the hot press ram displacement at ~1330 °C, which is close to the onset of melting in the Zr–Si binary.

The use of ZrB_2-based materials at high temperatures requires elimination of low melting phases. In this connection, it is worth noting that slightly longer processing times eliminate the need for Ni as observed in Fig. 2. However, we believe that even if Ni used, the small volume fractions (~0.5%) remaining as elemental metal unlikely to pose a problem.

5. Conclusions

Reactive hot pressing can be used to densify ZrB_2–SiC and ZrB_2–ZrC–SiC composites at temperature as low as 1600 °C to yield ~97–98% RD with or without Ni. Intermediate phases of ZrC and Zr–Si compounds precede the formation of the final products. Tailoring of the reaction mixture allows the SiC content to be increased to 30 vol% in ZrB_2–SiC composite with 96% RD. The densification appears to be driven partly by the presence of a transient ZrC phase and the fine sub-micron grain structure developed during the early stage of reaction. Additional factors that may help complete densification and induce coarsening at temperatures beyond 1350 °C include a transient liquid phase based on the Zr–Si eutectic. Nickel addition is not essential for densification.

Acknowledgements

The authors acknowledge the support from Director, NAL, Head, Materials Science Division, NAL and a grant to Indian Institute of Science from Defence Research and Development Organization. The authors thank Mr. V. Babu for assistance in hot pressing experiments, Dr. S. Usha Devi for XRD measurements and Mr. Keshab Barai for assistance in SEM work.

References

1. Kuriakose, A. K. and Margrave, J. L., The oxidation kinetics of zirconium diboride and zirconium carbide at high temperatures. *J. Electrochem. Soc.*, 1964, **111**(7), 827–831.
2. Tripp, W. C. and Graham, H., Thermogravimetric study of the oxidation of ZrB_2 in the temperature range of 800–1500 °C. *J. Electrochem. Soc.*, 1968, **118**(7), 1195–1199.
3. Irving, R. J. and Worsley, I. G., Oxidation of titanium diboride and zirconium diboride at high temperatures. *J. Less-Common Met.*, 1968, **16**(2), 102–112.
4. Tripp, W. C., Davis, H. H. and Graham, H. C., Effect of an SiC addition on the oxidation of ZrB_2. *Am. Ceram. Soc. Bull.*, 1973, **52**(8), 612–616.
5. Opila, E. and Halbig, M. C., Oxidation of ZrB_2–SiC. *Ceram. Eng. Sci. Proc.*, 1989, **10**(7–8), 221–228.
6. Levine, S. R., Opila, E. J., Halbig, M. C., Kiser, J. D., Singh, M. and Salem, J. A., Evaluation of ultra-high temperature ceramics for aeropropulsion use. *J. Eur. Ceram. Soc.*, 2002, **22**, 2757–2767.
7. Opeka, M. M., Talmy, I. G., Wuchina, E. J., Zaykoski, J. A. and Causey, S. J., Mechanical, thermal and oxidation properties of refractory hafnium and zirconium compounds. *J. Eur. Ceram. Soc.*, 1999, **19**, 2405–2414.
8. Chamberlain, A. L., Fahrenholtz, W., Hilmas, G. and Ellerby, D., Oxidation of ZrB_2–SiC ceramics under atmospheric and reentry conditions. *Refr. Appl. Trans.*, 2005, **1**(2), 1–8.
9. Opeka, M. M., Talmy, I. G. and Zaykoski, J. A., Oxidation-based materials selection for 2000 °C+ hypersonic aerosurfaces: theoretical consideration and historical experience. *J. Mater. Sci.*, 2004, **39**, 5887–5904.
10. Upadhya, K., Yang, J. M. and Hoffman, W. P., Materials for ultra-high temperature structural applications. *Am. Ceram. Soc. Bull.*, 1997, **76**(12), 51–56.
11. Gasch, M., Ellerby, D., Irby, E., Beckman, S., Gusman, M. and Johnson, S., Processing, properties and arc jet oxidation of hafnium diboride/silicon carbide ultra high temperature ceramics. *J. Mater. Sci.*, 2004, **39**, 5925–5937.
12. Scatteia, L., Riccio, A., Rufolo, G., De Filippis, F., Del Vecchio, A. and Marino, G., PRORA-USV SHS: ultra high temperature ceramic materials for sharp hot structure. In *AIAA/CIRA 13th International Space Planes and Hypersonics Systems and Technology AIAA 2005-3266*, 2005, pp. 1–16.
13. Mishra, S. K., Das, S., Das, S. K. and Ramachandrarao, P., Sintering studies on ultrafine ZrB_2 powder produced by a self-propagating high-temperature synthesis process. *J. Mater. Res.*, 2000, **15**(11), 2499–2504.
14. Mishra, S. K., Das, S. K., Ray, A. K. and Ramachandrarao, P., Effect of Fe and Cr addition on the sintering behavior of ZrB_2 produced by self-propagating high-temperature synthesis. *J. Am. Ceram. Soc.*, 2002, **85**(11), 2846–2848.
15. Chamberlain, A. L., Fahrenholtz, W. G. and Hilmas, G. E., Pressureless sintering of zirconium diboride. *J. Am. Ceram. Soc.*, 2006, **89**(2), 450–456.
16. Zhu, S., Fahrenholtz, W. G., Hilmas, G. E. and Zhang, S. C., Pressureless sintering of zirconium diboride using boron carbide and carbon additions. *J. Am. Ceram. Soc.*, 2007, **90**(11), 3660–3663.
17. Sciti, D., Brach, M. and Bellosi, A., Oxidation behavior of a pressureless sintered ZrB_2–$MoSi_2$ ceramic composite. *J. Mater. Res.*, 2005, **20**(4), 922–930.
18. Sciti, D., Guicciardi, S. and Bellosi, A., Properties of a pressureless-sintered ZrB_2–$MoSi_2$ ceramic composite. *J. Am. Ceram. Soc.*, 2006, **89**(7), 2320–2322.
19. Silvestroni, L. and Sciti, D., Effects of $MoSi_2$ additions on the properties of Hf- and Zr–B_2 composites produced by pressureless sintering. *Scripta Mater.*, 2007, **57**, 165–168.
20. Yan, Y., Huang, Z., Dong, S. and Jiang, D., Pressureless sintering of high-density ZrB_2–SiC ceramic composites. *J. Am. Ceram. Soc.*, 2006, **89**(11), 3589–3592.
21. Monteverde, F., Guicciardi, S. and Bellosi, A., Advances in microstructure and mechanical properties of ZrB_2 based ceramics. *Mater. Sci. Eng. A*, 2003, **A346**(1–2), 310–319.
22. Marschall, J., Erlich, D. C., Manning, H., Duppler, W., Ellerby, D. and Gasch, M., Microhardness and high-velocity impact resistance of HfB_2/SiC and ZrB_2/SiC composites. *J. Mater. Sci.*, 2004, **39**, 5959–5968.
23. Opila, E., Levine, S. and Lorincz, J., Oxidation of ZrB_2- and HfB_2-based ultra-high temperature ceramics: effect of Ta additions. *J. Mater. Sci.*, 2004, **39**, 5969–5977.
24. Fahrenholtz, W. G., Hilmas, G. E., Chamberlain, A. L. and Zimmermann, J. W., Processing and characterization of ZrB_2-based ultra-high temperature monolithic and fibrous monolithic ceramics. *J. Mater. Sci.*, 2004, **39**, 5951–5957.
25. Chamberlain, A. L., Fahrenholtz, W. G., Hilmas, G. E. and Ellerby, D. T., High strength zirconium diboride based ceramics. *J. Am. Ceram. Soc.*, 2004, **87**(6), 1170–1172.
26. Monteverde, F. and Bellosi, A., The resistance to oxidation of an HfB_2–SiC composite. *J. Eur. Ceram. Soc.*, 2004, **25**, 1025–1031.
27. Monteverde, F., The thermal stability in air of hot-pressed diboride matrix composites for uses at ultra-high temperature applications. *Corros. Sci.*, 2005, **47**, 2020–2033.
28. Monteverde, F. and Bellosi, A., Development and characterization of metal-diboride-based composites toughened with ultra-fine SiC particulates. *Solid State Ionics*, 2005, **7**, 622–630.
29. Monteverde, F., Beneficial effects of an ultra-fine α-SiC incorporation on the sinterability and mechanical properties of ZrB_2. *Appl. Phys. A*, 2006, **82**, 329–337.
30. Rezaie, A., Fahrenholtz, W. G. and Hilmas, G. E., Effect of hot pressing time and temperature on the microstructure and mechanical properties of ZrB_2–SiC. *J. Mater. Sci.*, 2007, **42**, 2735–2744.
31. Melendez-Martinez, J. J., Dominguez-Rodriquez, A., Monteverde, F., Melandri, C. and de Portu, G., Characterization and high temperature mechanical properties of zirconium diboride-based materials. *J. Eur. Ceram. Soc.*, 2002, **22**, 2543–2549.
32. Monteverde, F., Bellosi, A. and Guicciardi, S., Processing and properties of zirconium diboride-based composites. *J. Eur. Ceram. Soc.*, 2002, **22**, 279–288.
33. Zhang, G. J., Deng, Z. Y., Kondo, N., Yang, J. F. and Ohji, T., Reactive hot pressing of ZrB_2–SiC composites. *J. Am. Ceram. Soc.*, 2000, **83**(9), 2330–2332.
34. Zhang, G. J., Ando, M., Yang, J. F., Ohji, T. and Kanzaki, S., Boron carbide and nitride as reactants for in situ synthesis of boride-containing ceramic composites. *J. Eur. Ceram. Soc.*, 2004, **24**, 171–178.
35. Montverde, F., Progress in the fabrication of ultra-high-temperature ceramics: *in-situ* synthesis, microstructure and properties of reactive hot pressed HfB_2–SiC composite. *Comp. Sci. Technol.*, 2005, **65**, 1869–1879.
36. Wu, W. W., Zhang, G. J., Kan, Y. M. and Wang, P. L., Reactive hot pressing of ZrB_2–SiC–ZrC ultra high-temperature ceramics at 1800 °C. *J. Am. Ceram. Soc.*, 2006, **89**(9), 2967–2969.
37. Zimmermann, J. W., Hilmas, G. E., Fahrenholtz, W. G., Monteverde, F. and Bellosi, A., Fabrication and properties of reactively hot pressed ZrB_2–SiC ceramics. *J. Eur. Ceram. Soc.*, 2007, **27**, 2729–2739.
38. Chamberlain, A. L., Fahrenholtz, W. G. and Hilmas, G. E., Low-temperature densification of zirconium diboride ceramics by reactive hot pressing. *J. Am. Ceram. Soc.*, 2006, **89**(12), 3638–3645.
39. Medri, V., Monteverde, F., Balbo, A. and Bellosi, A., Comparison of ZrB_2–ZrC–SiC composites fabricated by spark plasma sintering and hot pressing. *Adv. Eng. Mater.*, 2005, **7**(3), 159–163.
40. Bellosi, A., Monteverde, F. and Scitti, D., Fast densification of ultra-high-temperature ceramics by spark plasma sintering. *Int. J. Appl. Ceram. Technol.*, 2006, **3**(1), 32–40.
41. Zhao, Y., Wang, L. J., Zhang, G. J., Jiang, W. and Chen, L. D., Preparation and microstructure of a ZrB_2–SiC composite fabricated by the Spark Plasma Sintering-Reactive Synthesis (SPS-RS) method. *J. Am. Ceram. Soc.*, 2007, **90**(12), 4040–4042.
42. Wu, W. W., Zhang, G. J., Kan, Y. M. and Wang, P. L., Reactive hot pressing of ZrB_2–SiC–ZrC composites. *J. Am. Ceram. Soc.*, 2008, **91**(8), 2501–2508.
43. Rangaraj, L., Suresha, S. J., Divakar, C. and Jayaram, V., Low temperature processing of ZrB_2–ZrC composites by reactive hot pressing. *Metall. Mater. Trans. A*, 2008, **39A**, 1496–1505.
44. Rangaraj, L., Divakar, C. and Jayaram, V., Reactive hot pressing of titanium nitride–titanium diboride composites at moderate pressure and temperatures. *J. Am. Ceram. Soc.*, 2004, **87**(10), 1872–1878.

45. Raju, G. B. and Basu, B., Densification, sintering reactions and properties of titanium diboride with titanium disilicide as sintering aid. *J. Am. Ceram. Soc.*, 2007, **90**(11), 3415–3423.
46. Barsoum, M. W. and Houng, B., Transient plastic phase processing of titanium–boron–carbon composites. *J. Am. Ceram. Soc.*, 1993, **76**(6), 1445–1451.
47. Williams, W. S., Influence of temperature, strain rate, surface condition and composition on the plasticity of transition-metal carbide crystals. *J. Appl. Phys.*, 1964, **35**(4), 1329–1338.
48. Alloy Phase Diagrams, *ASM Handbook*, *vol. 3*. ASM International, Materials Park, OH, 1992.